

Influence of Conduction Electrons on the Lattice Specific Heat and Elastic Moduli of Alpha-Phase Alloys of the Noble Metals*

J. G. COLLINS†

Institute for Atomic Research and Department of Physics, Iowa State University, Ames, Iowa

(Received 5 August 1966)

Measurements near 0°K of the lattice specific heat and the elastic moduli C_{ij} of α -phase alloys of the noble metals imply a change in Debye temperature Θ which is a function only of the electron/atom ratio when the solute is iso-electronic with the solvent. An attempt is made to estimate the variation in Θ by calculating the dependence of the shear moduli on the total kinetic energy of the electron system. The band structure is assumed rigid and the energy surfaces, which are defined using a nearly-free-electron model, are chosen so that the shape of the model Fermi surface resembles that which has been measured for the pure metals. The calculated variation with electron density is too large, particularly for C_{44} , and the observed change in Θ cannot be reproduced. This is probably due to the use of a rigid-band model, which predicts a *decrease* in the density of states with increasing electron/atom ratio for a Fermi surface which contacts the zone boundary, and is consequently unable to explain the observed changes in either the lattice or the electronic heat capacities.

I. INTRODUCTION

THE heat capacity C_v of a metal at very low temperatures ($T \lesssim 4.2^\circ\text{K}$) can be analyzed into two principal contributions;

$$C_v \approx \gamma T + (12\pi^4/5)N_0k(T/\Theta)^3 + O(T^5). \quad (1)$$

The term linear in T is the specific heat of the conduction electrons and the coefficient γ is directly proportional to the density of electron states at the Fermi surface $N(E_F)$. The cubic term arises from long-wavelength thermal vibrations of the lattice, the physical properties of which are characterized by the Debye temperature Θ . (The symbols N_0 and k are Avagadro's and Boltzmann's constants, respectively, and throughout the paper Θ means the Debye temperature at $T=0^\circ\text{K}$). At very low temperatures a solid behaves like an elastic continuum for which Θ may be related to an average velocity of sound and hence to an average elastic modulus \bar{C} . If we neglect various constants, we can write

$$\Theta \propto (\bar{C}/\rho a^2)^{1/2}, \quad (2)$$

where a is the lattice constant and ρ is the density of the solid. Details of the averaging procedure are given, for example, in the review by Blackman.¹ Here we merely wish to point out the functional relationship between the Debye temperature and the elastic moduli.

The specific heats at low temperature of Cu, Ag, and Au and of a number of their α -phase alloys have been measured very precisely over the past ten years.²⁻⁷

Interest has centered mainly on the change in γ/γ_0 with change in the electron/atom ratio (e/a) of the alloy.⁸ The majority of the experimental points suggest that as e/a increases the electronic density of states in these alloys rises steadily, but at a slower rate than would be expected for a distribution of free electrons. This is in apparent defiance of all theories based on a "rigid-band" extension of the known properties of electrons at the Fermi surface of the pure solvents, and has not yet been satisfactorily explained.⁹ The present paper has nothing to offer on this puzzling question beyond presenting a further theoretical density-of-states curve based on a rigid-band model (see Fig. 7). Here we are primarily concerned with a similar trend with e/a in the lattice heat capacity of these alloys. The ratio of the Debye temperature Θ of an alloy to the value Θ_0 for the pure solvent appears to be (a) a function only of the e/a ratio of the alloy, and (b) independent of the nature of the solvent, for solutes whose ion cores are iso-electronic with the solvent, i.e., for Ni, Zn, Ga, Ge, and As in Cu and for Pd, Cd, In, Sn, and Sb in Ag.

The elastic moduli of a number of these alloy systems have also been measured.¹⁰⁻¹³ Rayne's measurements on copper based alloys extend from room temperature down to 4.2°K, while those by Smith and his co-workers are at room temperature only. We have scaled the latter results to low temperatures according to the measured ratio of low-temperature to room-temperature

* J. A. Birch and G. K. White (private communication); H. Montgomery and G. P. Pells (private communication to J. A. Birch and G. K. White).

⁷ B. A. Green, Jr., and H. V. Culbert, *Phys. Rev.* **137**, 1168 (1965).

⁸ Throughout the paper the subscript zero refers to the pure solvent metal.

⁹ See, for example, J. M. Ziman, *Advan. Phys.* **10**, 1 (1961); H. Jones, *Phys. Rev.* **134**, A958 (1964); *Proc. Roy. Soc. (London)* **A294**, 405 (1966); A. D. Brailsford, *ibid.* **A292**, 433 (1966); P. G. Dawber and R. E. Turner, *Proc. Phys. Soc. (London)* **88**, 217 (1966).

¹⁰ J. R. Neighbours and C. S. Smith, *Acta Met.* **2**, 591 (1954).

¹¹ R. Bacon and C. S. Smith, *Acta Met.* **4**, 337 (1956).

¹² R. E. Schmunk and C. S. Smith, *Acta Met.* **8**, 396 (1960).

¹³ J. A. Rayne, *Phys. Rev.* **115**, 63 (1959).

* Work was performed in part at the Ames Laboratory of the U. S. Atomic Energy Commission. Contribution No. 1941.

† Division of Physics, Commonwealth Scientific and Industrial Research Organization, Sydney, Australia.

¹ M. Blackman, in *Handbuch der Physik*, edited by S. Flügge (Springer-Verlag, Berlin, 1955), Vol. VII/1, p. 325.

² J. A. Rayne and W. R. G. Kemp, *Australian J. Phys.* **9**, 569 (1956).

³ J. A. Rayne, *Phys. Rev.* **110**, 606 (1958).

⁴ B. W. Veal and J. A. Rayne, *Phys. Rev.* **130**, 2156 (1963).

⁵ L. L. Isaacs and T. B. Massalski, *Phys. Rev.* **138**, A134 (1965); T. B. Massalski and L. L. Isaacs, *ibid.* **138**, A139 (1965).

values for the pure solvents,¹⁴ and have calculated a Debye temperature for each alloy using de Launay's interpolation tables.¹⁵

The reduced temperature ratio $\Theta(\rho a^2)^{1/2}/\Theta_0(\rho a^2)_0^{1/2} = (\bar{C}/\bar{C}_0)^{1/2}$, in which allowance has been made for the explicit dependence of Θ on the density and lattice spacing of the alloys,^{16,17} is plotted in Fig. 1 using all available heat-capacity and elastic measurements. The steady and approximately linear drop in Θ/Θ_0 derived from both the heat-capacity and the elastic measurements has been commented on by various authors but, apart from some work by Rayne,³ no attempt has been made to explain it quantitatively.

In the present paper the observed variation of the elastic moduli and hence of Θ/Θ_0 is assumed to be due solely to a change with alloying in the contribution of the conduction electrons to the elastic moduli. We set up a rigid-band model of the electronic energy-momentum relation and fix all arbitrary parameters so as to give agreement for the pure solvent (a) between the gross features of the model Fermi surface and the Fermi surface which has been deduced from de Haas-van Alphen measurements,¹⁸ and (b) between the measured and calculated elastic shear moduli. The model is then used to predict the elastic moduli when the e/a ratio changes from unity, and to compare these with the measured values for the alloy systems.

Two important qualifications to this program should be pointed out. Firstly, we calculate the elastic moduli for a constant lattice spacing and so assume that there

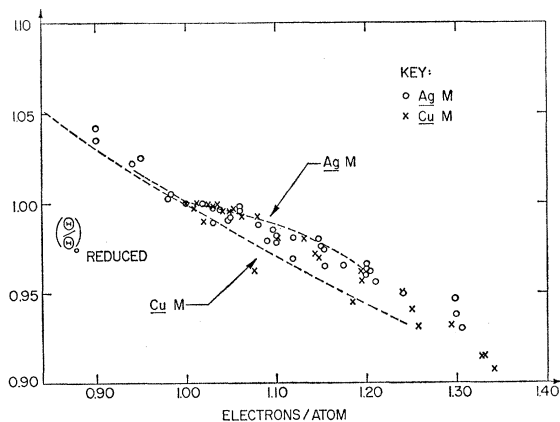


FIG. 1. The relative variation with e/a ratio of the Debye temperature of α -phase alloys of Cu and of Ag. The points are taken directly from heat capacity measurements (see Refs. 2-7) and the broken lines are calculated from measurements of the elastic moduli (see Refs. 10-13). "Reduced" means that the explicit dependence of Θ on density and on lattice constant has been removed using Eq. (2).

¹⁴ J. R. Neighbours and G. A. Alers, *Phys. Rev.* **111**, 707 (1958).

¹⁵ J. de Launay, *Solid State Phys.* **2**, 220 (1956).

¹⁶ W. B. Pearson, *Handbook of Lattice Spacings and Structures of Metals* (Pergamon Press, Ltd., London, 1958).

¹⁷ For these iso-electronic sequences the net density and lattice constant variation changes Θ/Θ_0 by less than 1%.

¹⁸ D. J. Roaf, *Phil. Trans. Roy. Soc. London* **A255**, 135 (1962).

is no difference in the sizes of the ion cores of solvent and iso-electronic solutes, i.e., we assume that alloying changes *only* e/a and does not affect the exchange repulsion between cores. To relax this condition would require a further assumption about the exchange interaction and another arbitrary parameter, and this we wish to avoid. As a consequence we do not include the recent heat-capacity measurements by Green and co-workers¹⁹ on CuSn and AgZn systems. These alloys show large variations in lattice constant from the pure metal, indicating large differences in the sizes of the ion cores, and the reduced Θ/Θ_0 lie, respectively, slightly below and above the general line of the points in the figure. Secondly, we do not calculate the variation in bulk modulus of the alloys, since this requires a knowledge of the second-order dependence of the size and shape of the Fermi surface upon volume. Templeton²⁰ has observed the de Haas-van Alphen effect in the noble metals under pressure, but his measurements can be interpreted in terms of only a first-order variation with volume in the size of the necks and hence in the shape of the Fermi surface.²¹ We therefore restrict our attention to the elastic shear moduli and to elastic strains which do not change the volume of the solid.

In Sec. II we outline the method used to calculate the elastic constants as derivatives of contributions to the elastic deformation energy from both lattice and electrons. The model used to represent the Brillouin zone and the electron energy-momentum relation is then defined, and all of its parameters fixed by comparison with the measured Fermi-surface geometry of the pure solvent metals. Computed values of the shear moduli are given in Sec. IV, after which the numerical results and the physical implications of the calculation are assessed.

II. ELASTIC SHEAR MODULI

The elastic strain energy W of the face-centered-cubic (fcc) lattice is given by the equation

$$W = W_0 + \frac{1}{2}C_{11}(\eta_1^2 + \eta_2^2 + \eta_3^2) + C_{12}(\eta_1\eta_2 + \eta_2\eta_3 + \eta_3\eta_1) + \frac{1}{2}C_{44}(\eta_4^2 + \eta_5^2 + \eta_6^2), \quad (3)$$

where C_{ij} are the three independent elastic moduli, η_1 , η_2 , and η_3 are the diagonal elements of the strain tensor $\boldsymbol{\eta}$, and $\frac{1}{2}\eta_4$, $\frac{1}{2}\eta_5$, and $\frac{1}{2}\eta_6$ are the off-diagonal elements of $\boldsymbol{\eta}$. We use Voigt's notation.

The two most convenient shear moduli to consider are $\frac{1}{2}(C_{11} - C_{12}) \equiv C'$ and $C_{44} \equiv C$, and these can be calculated as second derivatives of W with respect to the appropriate strains. If the direct lattice is compressed along the z axis and allowed to expand equally along the x and y axes so as to maintain constant volume, the

¹⁹ L. C. Clune and B. A. Green, Jr., *Phys. Rev.* **144**, 525 (1966); B. A. Green, Jr., *ibid.* **144**, 528 (1966).

²⁰ I. M. Templeton, *Proc. Roy. Soc. (London)* **A292**, 413 (1966).

²¹ J. G. Collins, *Ann. Acad. Sci. Fennicae, Ser. A.VI.* **210**, 241 (1966).

strained lattice is described by vectors $\mathbf{r}' = (\mathbf{I} + \boldsymbol{\eta}) \cdot \mathbf{r}$, where

$$\mathbf{I} + \boldsymbol{\eta} = \begin{bmatrix} (1+\epsilon)^{-1/2} & 0 & 0 \\ 0 & (1+\epsilon)^{-1/2} & 0 \\ 0 & 0 & 1+\epsilon \end{bmatrix}. \quad (4)$$

It follows that

$$C' = \frac{1}{3}(\partial^2 W / \partial \epsilon^2)_{\epsilon=0}. \quad (5)$$

Again, if the direct lattice is strained at constant volume by a tension in the (101) direction, the new lattice vectors are $\mathbf{r}' = (\mathbf{I} + \boldsymbol{\eta}) \cdot \mathbf{r}$, where now

$$\mathbf{I} + \boldsymbol{\eta} = (1 - \frac{1}{4}\gamma^2)^{-1/3} \begin{bmatrix} 1 & 0 & \frac{1}{2}\gamma \\ 0 & 1 & 0 \\ \frac{1}{2}\gamma & 0 & 1 \end{bmatrix}, \quad (6)$$

and the appropriate elastic constant is

$$C = (\partial^2 W / \partial \gamma^2)_{\gamma=0}. \quad (7)$$

We consider the total elastic strain energy W of the solid to be made up of three additive contributions: W_E arises from electrostatic interactions between ions immersed in a sea of electrons which maintains over-all charge neutrality; W_R is the energy from exchange repulsion between neighboring ion cores; and W_F is the total kinetic energy of the electrons which we will refer to as the Fermi energy. It follows immediately that the elastic shear moduli also have three components;

$$\begin{aligned} C &= C_E + C_R + C_F, \\ C' &= C_E' + C_R' + C_F'. \end{aligned} \quad (8)$$

A. Electrostatic Terms

Thirty years ago, Fuchs²² calculated C_E and C_E' for a fcc lattice of positive ions each with charge Ze in a uniform background of electrons. His result was

$$\begin{aligned} C_E &= 0.9479Z^2e^2/\frac{1}{2}a^4 \text{ dyn cm}^{-2}, \\ C_E' &= 0.1058Z^2e^2/\frac{1}{2}a^4 \text{ dyn cm}^{-2}. \end{aligned} \quad (9)$$

In a metal the electron density is not constant over the unit cell and in an alloy the valency Z varies between cells which suggests that Fuchs's formulas should be modified. Specific procedures for the calculation of an effective valency Z_{eff} have been given, for example, by Leigh²³ and by Huntington²⁴ to allow for this non-uniformity of the charge density. Arguments about the extent of electron screening of impurity ions and the associated long-range fluctuations in electron density are also relevant here.²⁵ We take Z to be the mean valency of the ions, i.e., $Z = e/a$. This is consistent with the assumption underlying this whole calculation,

²² K. Fuchs, Proc. Roy. Soc. (London) **A153**, 622 (1936); **A157**, 444 (1936).

²³ R. S. Leigh, Phil. Mag. **42**, 139 (1951).

²⁴ H. B. Huntington, Solid State Phys. **7**, 213 (1958).

²⁵ See, for example, J. M. Ziman, Advan. Phys. **13**, 89 (1964).

namely, that a rigid-band model can be used to describe the band structure, for this implies perfect uniformity between unit cells in the direct lattice and hence a uniform ionic charge distribution. Also we are considering alloys with up to 35-at.-% solute, and when every third or fourth ion is an impurity, it is surely incorrect to consider them as being independently screened by the electrons. The screening problem becomes completely nonlinear and the simple assumption of a uniform density of electrons may again be valid. Whether Z is taken to be always unity, as has been suggested, or equal to e/a does not matter a great deal numerically here because of the predominance of the repulsive and Fermi contributions.

B. Exchange Terms

We represent the ion-ion exchange repulsion by an energy of interaction $W_R(r)$ between any pair of ions a distance r apart. Then the contributions to the shear moduli from nearest neighbors in a fcc lattice are

$$\begin{aligned} C &= r^2 d^2 W_R / dr^2 + 3r(dW_R/dr), \\ C' &= \frac{1}{2}r^2 d^2 W_R / dr^2 + \frac{1}{2}r(dW_R/dr). \end{aligned} \quad (10)$$

We make no specific assumptions about the form of $W_R(r)$, but treat the two derivatives dW_R/dr and d^2W_R/dr^2 as parameters to be fitted using the measured shear moduli of the pure solvent metal and then kept constant when the metal is alloyed, i.e., we assume identical ion cores for the isoelectronic sequences. Interactions between more distant neighbors are neglected.

C. Fermi Terms

The Fermi energy of the electron distribution is

$$W_F = \int_0^{E_F} N(E) E dE, \quad (11)$$

where $N(E)$ is the density of states and E_F is the Fermi level. For a completely free-electron system with a spherical Fermi surface and no zone boundaries, W_F is independent of all strains which conserve volume and the electrons do not contribute to the shear moduli. In the past this has been assumed to be the case for the noble metals and previous theoretical treatments for Cu, Ag, and Au have always neglected contributions from the conduction electrons to the shear moduli (e.g. Refs. 10–12.) But we have known since 1957 that the Fermi surface in Cu,²⁶ and, more recently,¹⁸ in Ag and Au, is greatly distorted from spherical and contacts the zone boundary over an appreciable area in the {111} directions. It follows that the Fermi energy is a function of strain and will in general contribute to the shear

²⁶ A. B. Pippard, Phil. Trans. Roy. Soc. London **A250**, 325 (1957).

moduli. In Eq. (11) above, both the Fermi level E_F and the density of states N are strain-dependent.

The treatment given here follows very closely those of Leigh,²³ who in 1951 calculated the contribution to the elastic constants of Al from the conduction electrons, and of Jones,²⁷ who made a similar calculation for β brass. Whereas Leigh at that time had no explicit information about the Fermi surface of Al and was forced to assume an arbitrary $E(\mathbf{k})$ relation, we are now in a position to make a similar calculation for the noble metals for which the topology of the Fermi surface is well established. The details of the model zone structure which is used are given in the following sections; here we establish the formal equations required to evaluate C_F and $C_{F'}$ from W_F .

When the metal is sheared at constant volume, the density of electrons per atom n remains constant and the Fermi level, though it may change, remains uniform over the Fermi surface. At the same time, depending upon the type of shear applied, the eight hexagonal and six square faces of the Brillouin zone all change their distances p from the origin of reciprocal space by differing amounts. A change in p in turn leads to a change in the distance of the Fermi surface from the zone boundary and hence to a change in shape of the Fermi surface. In what follows, therefore, we must treat separately the electrons in each of the 14 segments of the zone defined by the 14 faces, and then sum to find the total changes in the electron distribution and in the Fermi energy caused by the shear.

Following Leigh, we define an index i which refers to faces of either hexagonal or square shape, and a second index j which refers to a particular face within the hexagonal or square group. Then, if E is the Fermi level, we can write

$$n = \sum_i \sum_j n_{ij} = \sum_i \sum_j \int_0^{E(p_{ij})} N_{ij}(E(p_{ij}), p_{ij}) dE, \quad (12)$$

where we allow the density of states to be both an explicit and an implicit function of p in each segment of the zone. We require second derivatives of the Fermi energy W_F with respect to a strain parameter x taken at constant electron density n . These may be evaluated in terms of partial derivatives of W_F and n with respect to x taken at constant Fermi level E as follows.

We express the constancy of the electron density by the equation

$$\frac{dn}{dx} = 0 = N(E) \frac{dE}{dx} + \sum_i \frac{dn_{ij}}{dp_{ij}} \sum_i \frac{dp_{ij}}{dx}. \quad (13)$$

(The formal dependence of n_{ij} on p_{ij} is independent of j , and all derivatives are evaluated at zero strain.) The variation of a reciprocal lattice vector \mathbf{g} ($|\mathbf{g}| = 2p$) with

strain is found by using the appropriate inverse transformations

$$\mathbf{g}' = \mathbf{g} \cdot (\mathbf{I} + \boldsymbol{\eta})^{-1} \quad (14)$$

for C and C' shear. It then follows from the volume-conservation condition that: for C shear

$$\sum \left(\frac{dp}{dx} \right)_{\text{hex}} = 0, \quad \left(\frac{dp}{dx} \right)_{\text{square}} = 0; \quad (15)$$

for C' shear

$$\left(\frac{dp}{dx} \right)_{\text{hex}} = 0, \quad \sum \left(\frac{dp}{dx} \right)_{\text{square}} = 0.$$

There is consequently no first-order change in the Fermi level and

$$dE/dx = 0. \quad (16)$$

There is, however, a second-order change in the Fermi level and this is found by setting the total second derivative of n with respect to x equal to zero. We get

$$\begin{aligned} \frac{d^2 E}{dx^2} &= -\frac{1}{N(E)} \left(\frac{\partial^2 n}{\partial x^2} \right)_E \\ &= -\frac{1}{N(E)} \sum_i \left[\frac{d^2 n_{ij}}{dp_{ij}^2} \sum_i \left(\frac{dp_{ij}}{dx} \right)^2 + \frac{dn_{ij}}{dp_{ij}} \sum_i \frac{d^2 p_{ij}}{dx^2} \right]. \end{aligned} \quad (17)$$

If we now differentiate the Fermi energy

$$W_F = \sum_i \sum_i \int_0^E N(E) E dE \quad (18)$$

twice with respect to x and incorporate the above results, we find

$$dW_F/dx = 0, \quad (19)$$

and

$$\begin{aligned} (d^2 W_F/dx^2)_n &= (\partial^2 W_F(p)/\partial x^2)_E - E(\partial^2 n(p)/\partial x^2)_E \\ &= (\partial^2 \bar{W}_F(p)/\partial x^2)_E, \end{aligned} \quad (20)$$

where $\bar{W}_F = W_F - En$.

Since we know how p depends on strain, we can finally express C_F and $C_{F'}$ as derivatives of \bar{W}_F with respect to p . If w_F is the contribution to \bar{W}_F from one segment of the zone, we have

$$\begin{aligned} C_F &= \left[\frac{16}{9} p \frac{\partial w}{\partial p} + \frac{8}{9} p^2 \frac{\partial^2 w}{\partial p^2} \right]_{\text{hex}} + \left[2p \frac{\partial w}{\partial p} \right]_{\text{square}}, \\ C_{F'} &= \left[\frac{8}{3} p \frac{\partial w}{\partial p} \right]_{\text{hex}} + \left[p \frac{\partial w}{\partial p} + p^2 \frac{\partial^2 w}{\partial p^2} \right]_{\text{square}}, \end{aligned} \quad (21)$$

where the subscripts refer to the two types of zone face.

As Jones²⁷ has pointed out, these equations have the same structure as those for C_R and $C_{R'}$ for a body-centered-cubic (bcc) lattice with nearest and next-

²⁷ H. Jones, Phil. Mag. 43, 105 (1952).

nearest neighbor interaction. The Fermi energy $W_F(p)$ arises from a central force interaction in reciprocal space because we have chosen $p = \frac{1}{2} |g|$ as the strain-dependent variable which governs the energy-band structure. This is shown explicitly in Sec. III.

III. MODEL BRILLOUIN ZONE

We define a set of energy surfaces in momentum space using the approximation of nearly-free electrons. We further assume that the surfaces within each segment of the Brillouin zone are axially symmetric about the reciprocal lattice vector through that segment and thus approximate the true zone by a series of cones based on the zone faces. With this assumption, the energy surfaces within each cone can be specified in terms of a single variable, and the complete calculation including the double differentiation of the Fermi energy can be carried out analytically. The model Brillouin zone for the fcc structure is therefore made up of eight cones based on the hexagonal {111} faces and six cones based on the square {200} faces. This "8-6 cone" model is closely related to the "8-cone" model used by Ziman⁹ in a review of the transport properties of the noble metals. Ziman has discussed the cone model at length and reference should be made to his paper for fuller details of the formulas used below. Figure 2 defines the important parameters of the reciprocal space geometry.

We choose the wave function of an electron in state \mathbf{k} to be a linear combination of two plane waves with wave vectors \mathbf{k} and $(\mathbf{k} + \mathbf{g})$, where \mathbf{g} is the reciprocal lattice vector through the zone face nearest to \mathbf{k} , i.e.,

$$\psi_{\mathbf{k}} = \alpha_{\mathbf{k}} e^{i\mathbf{k} \cdot \mathbf{r}} + \beta_{\mathbf{k}} e^{i(\mathbf{k} + \mathbf{g}) \cdot \mathbf{r}}. \quad (22)$$

The energy $E_{\mathbf{k}}$ is then

$$E_{\mathbf{k}} = \frac{1}{2} [E_{\mathbf{k}^0} + E_{\mathbf{k} + \mathbf{g}^0} \pm ((E_{\mathbf{k} + \mathbf{g}^0} - E_{\mathbf{k}^0})^2 + 4V_g^2)^{1/2}], \quad (23)$$

where

$$E_{\mathbf{k}^0} = \hbar^2 k^2 / 2m, \quad (24)$$

and V_g is half of the energy band gap across the center of the zone face. Physically, V_g is the Fourier coefficient of some effective potential seen by the electrons, but we regard it as a parameter which governs the departure from sphericity of the energy surfaces within a cone, and which is to be fixed by reference to the known shapes of the Fermi surfaces of Cu, Ag, and Au. Since we are using two sets of cones to constitute the model zone, there are two parameters V_{111} and V_{200} to be fitted. The fitting procedure is described below.

It is convenient to calculate the electron densities and energies in terms of the following dimensionless quantities using $p = \frac{1}{2} |g|$ as the scaling parameter for each cone:

$$\begin{aligned} (x, y, z) &= \mathbf{k} / p, \\ U_g &= V_g / (\hbar^2 p^2 / m), \\ \mathcal{E} &= E_{\mathbf{k}} / (\hbar^2 p^2 / m) \\ &= \frac{1}{2} \{ x^2 + y^2 + 1 + (1 - z)^2 - 2((1 - z)^2 + U_g^2)^{1/2} \} \\ &= \frac{1}{2} \{ z_1^2 \tan^2 \alpha + 1 + (1 - z_1)^2 - 2((1 - z_1)^2 + U_g^2)^{1/2} \} \\ &= \frac{1}{2} \{ 1 + (1 - z_2)^2 - 2((1 - z_2)^2 + U_g^2)^{1/2} \}. \end{aligned} \quad (25)$$

The last equation defines the projections z_1 and z_2 of the surface $E_{\mathbf{k}}$ on the cone axis (see Fig. 2). The density of states N per unit volume per unit energy range, the density n of electrons per atom, and the Fermi energy W_F are then given by

$$\begin{aligned} N &= \frac{m p}{2\pi^2 \hbar^2} \sum_{\text{cones}} (z_2 - z_1), \\ n &= \frac{3\pi\sqrt{3}}{16} \sum_{\text{cones}} \left[\frac{1}{3} z_1^2 \tan^2 \alpha + (2\mathcal{E} - 1)(z_2 - z_1) + \frac{1}{3}(1 - z_2)^3 - \frac{1}{3}(1 - z_1)^3 - (1 - z_2)((1 - z_2)^2 + U_g^2)^{1/2} \right. \\ &\quad \left. + (1 - z_1)((1 - z_1)^2 + U_g^2)^{1/2} + U_g^2 \ln \frac{1 - z_1 + ((1 - z_1)^2 + U_g^2)^{1/2}}{1 - z_2 + ((1 - z_2)^2 + U_g^2)^{1/2}} \right], \end{aligned} \quad (26)$$

$$\begin{aligned} W_F &= \frac{\hbar^2 p^5}{8\pi^2 m} \sum_{\text{cones}} \left[2(\mathcal{E}^2 - U_g^2)z - \frac{1}{2}z + \frac{1}{10}(1 - z)^5 + (1 - z)^3 - \frac{1}{2}(1 - z)((1 - z)^2 + U_g^2)^{3/2} \right. \\ &\quad - (1 - \frac{1}{4}U_g^2) \{ (1 - z)((1 - z)^2 + U_g^2)^{1/2} + U_g^2 \sinh^{-1} \{ (1 - z)/U_g \} \}_{z_1^2} + \frac{1}{10}z_1^5 \tan^4 \alpha + \tan^2 \alpha \{ \frac{1}{3}z^3 - \frac{1}{3}z^2(1 - z)^3 \\ &\quad - \frac{1}{6}z(1 - z)^4 - (1/30)(1 - z)^5 + (1 - \frac{1}{4}U_g^2) \} \{ (1 - z)((1 - z)^2 + U_g^2)^{1/2} \\ &\quad \left. + U_g^2 \sinh^{-1} \{ (1 - z)/U_g \} \} - \frac{1}{6}(5 + 3z)((1 - z)^2 + U_g^2)^{3/2} \right]. \end{aligned}$$

In this last equation the expressions are to be evaluated at the limits z_2 , z_1 , and $z_1, 0$ as indicated by the superscripts and subscripts. Finally, where the Fermi surface contacts the zone boundary the radius r of the circle of

contact is given by

$$r^2 = p^2 (2\mathcal{E} + 2U_g - 1). \quad (27)$$

The mathematical procedure is as follows: The semi-

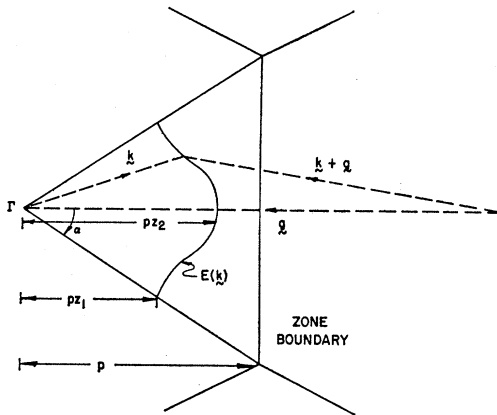


FIG. 2. Parameters which define the reciprocal space geometry of the model. One segment only of the zone is shown in cross section.

angle α of each cone is chosen so that the base of the cone is equal in area to, and lies in the same plane as, the zone face which it replaces. With this criterion the total volume and total solid angle of the model zone are within parts in 10^3 of 2 electrons/atom and 4π sr, respectively, and the maximum overlap of neighboring cones is only 3 to 4 degrees of arc. Agreement between these gross features of the model zone and the true zone is much better in all respects than with the simpler 8-cone model in which the six $\{200\}$ segments are absorbed into the neighboring $\{111\}$ cones. The two parameters V_{111} and V_{200} are then fixed by requiring that the energy surface in the model zone which just contains one e/a should also have a neck radius r at the $\{111\}$ zone boundary and a Fermi radius k_{200} equal to those measured experimentally for the noble metals. In practice, contours of constant r and k_{200} can be plotted for $n=1$ on a grid of (V_{111}, V_{200}) points and a solution found for each metal by interpolation. The choice of V_{111} and V_{200} is unique, but there is some uncertainty in V_{200} which is very sensitive to variations in the published experimental values of k_{200} . Figures for each metal are given in Table I.

With V_{111} and V_{200} fixed and kept constant (rigid band assumption) a complete set of energy surfaces is

TABLE I. Parameters used to define the energy surfaces in the model zone. Band gaps V_{111} and V_{200} are chosen to make the model Fermi surface for pure Cu, Ag, and Au fit the measured neck radius r and Fermi radius k_{200} . Distances from the zone center to the zone faces are p_{111} and p_{200} .

	r/p_{111}	k_{200}/p_{200}	V_{111}	V_{200}
Cu ^a	0.162–0.180	0.805–0.844	0.235 ± 0.02 (4.06 eV)	0.330 ± 0.03 (5.70 eV)
Ag ^a	0.122–0.128	0.805–0.836	0.200 ± 0.01 (2.70 eV)	0.295 ± 0.03 (3.99 eV)
Au ^a	0.160–0.171	0.836–0.883	0.245 ± 0.01 (3.31 eV)	0.365 ± 0.02 (4.94 eV)

^a See Ref. 18.

defined by Eq. (25) for each metal and its alloys, the position of the Fermi level for each being fixed by the e/a ratio. Figure 3 is a cross section of three cones showing the shape of the energy surfaces given by this model, while Fig. 4 shows the density of states for each system as a function of e/a . If x is the electron/atom ratio, we note that $d \ln N / d \ln x$ at $x=1$ is still negative, in apparent contradiction to the behavior deduced from measurements of the electronic heat capacities, and that there is a second cusp in the curves near the x value at which the α/β phase boundary occurs. This agrees with a recent suggestion by Hume-Rothery and Roaf²⁸ that the phase transition might occur when the Fermi surface is about to contact the $\{200\}$ faces of the Brillouin zone.

The remainder of the calculation is a straightforward but tedious analytical evaluation of C_F and C_F' in terms of the derivatives of W_F and of n with respect to p using Eqs. (21)–(27). Although shear strains change the sizes of p_{111} and p_{200} and hence both the position and shape of the energy surfaces, we assume that they do not affect the parameters V_{111} and V_{200} .

IV. SHEAR MODULI

A. General Remarks

When the lattice is strained, the position of the Fermi level and the shape of the energy surfaces change as various zone faces approach or recede from the zone center. Electrons redistribute themselves in reciprocal space so as to fill up again the states of lowest energy, and this in general causes a change in the Fermi energy and so contributes to the elastic moduli.

The C shear defined in Eq. (4) causes first-order shifts in the distances of the $\{111\}$ zone faces from the zone center but only second-order shifts in the positions of the $\{200\}$ faces. As a consequence, the value of C_F is governed largely by the behavior of electrons in energy levels near the $\{111\}$ faces and hence by the size of V_{111} . It is relatively insensitive to V_{200} . This is illustrated in Fig. 5(a), where C_F is plotted as a function of x

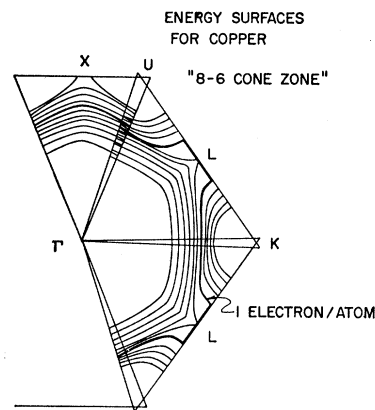


FIG. 3. Typical surfaces of constant energy in the cone model of the zone. The heavy line shows the surface which contains one electron/atom; the other surfaces are drawn at intervals of 0.1 e/a atom.

²⁸ W. R. Hume-Rothery and D. J. Roaf, *Phil. Mag.* **6**, 55 (1961).

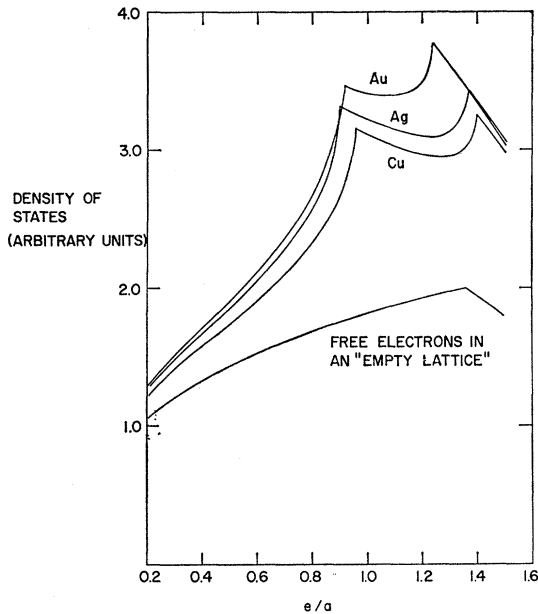


FIG. 4. Density-of-states curves for Cu, Ag, and Au lattices shown as functions of the e/a ratio and calculated using the 8-6 cone model.

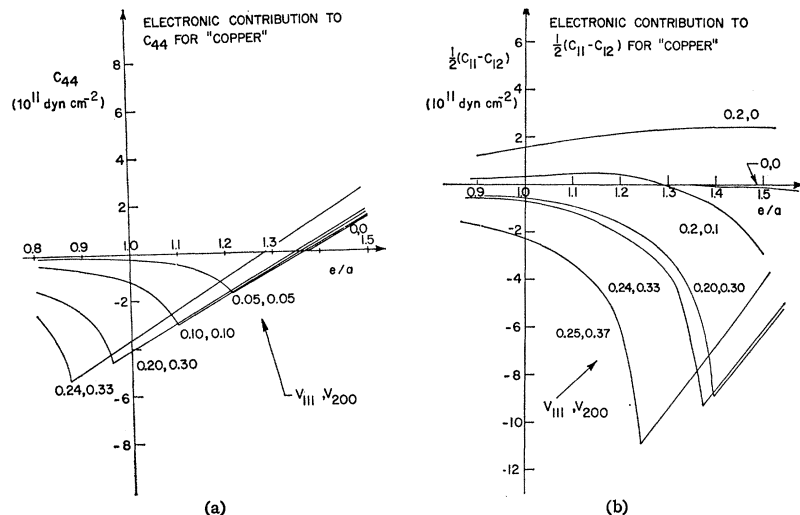
for various values of V_{111} and V_{200} for a metal with the lattice constant of copper. When both parameters are zero we have a sphere of free electrons in an empty lattice, i.e., a reciprocal lattice with no energy discontinuities at the zone faces, and there can be no contribution to the shear modulus until the sphere touches the zone boundary. This happens when $x \sim 1.38$ in a face-centered lattice. Thereafter, C strain increases the Fermi energy W_F as electrons redistribute around the truncated Fermi surface, and the contribution C_F is positive. This was the case studied by Rayne³ and the present calculation agrees with his result.

For electrons which are not free, the net effect of the movement of the $\{111\}$ faces before contact occurs is to

make available to the electrons regions of the surface with an increasingly higher density of states. The energy W_F decreases and C_F is negative. After a cusp at the value of x at which contact occurs, C_F becomes increasingly positive and, in fact, follows very closely an extension of the empty-lattice behavior. That is, once the Fermi surface has contacted the zone boundary, it is the area of contact rather than any precise details of the level structure which determines the elastic response. Distortion of the energy surfaces is only of secondary importance. The over-all shape of the C_F -versus- x curve reflects the inverted density-of-states curve in so far as it is affected by the $\{111\}$ faces; contact with the $\{200\}$ faces at higher x has virtually no effect on C_F , whereas it causes a second cusp to appear in $N(E)$.

The general trend of C_F' as a function of the shape of the Fermi surface is less clear cut [Fig. 5(b)]. The C' shear of Eq. (6) produces first-order changes in the positions of the $\{200\}$ faces and second-order changes in the positions of the $\{111\}$ faces, so that we expect the controlling influence on C_F' to be the $\{200\}$ faces (and this is, of course, why the 8-6 cone model is needed rather than the simpler 8-cone model). But the vastly increased contribution to N from energy states near the $\{111\}$ faces when there is contact or near contact counterbalances the second-order shift of the zone faces, and the net result can be either a positive or a negative C_F' depending upon the precise values of V_{111} and V_{200} . Again the empty lattice case shows no contribution to C' until $x \sim 1.38$; thereafter there is a small negative C_F' which is initially quadratic in $(x - 1.38)$. This is again in agreement with Rayne,³ who found C_F' to be zero to first order. As the Fermi surface approaches the $\{200\}$ faces, C_F' becomes increasingly negative with a cusp at contact and thereafter increases algebraically as does C_F . In this region, C_F' reflects an inversion of the cusp in the density-of-states curve due to the $\{200\}$ faces.

FIG. 5. Contributions to the shear moduli from the conduction electrons calculated using the 8-6 cone model for a metal with the lattice constant of Cu, plotted as a function of e/a ratio for various choices of the pair of parameters (V_{111}, V_{200}). Curves show how C_F and C_F' vary with the amount of distortion of the Fermi surface from a sphere. The curve (0.24, 0.33) corresponds to Cu itself while (0.20, 0.30) gives the value for Ag if the ordinate scale is multiplied by $(a_{Cu}/a_{Ag})^3 = 0.54$.



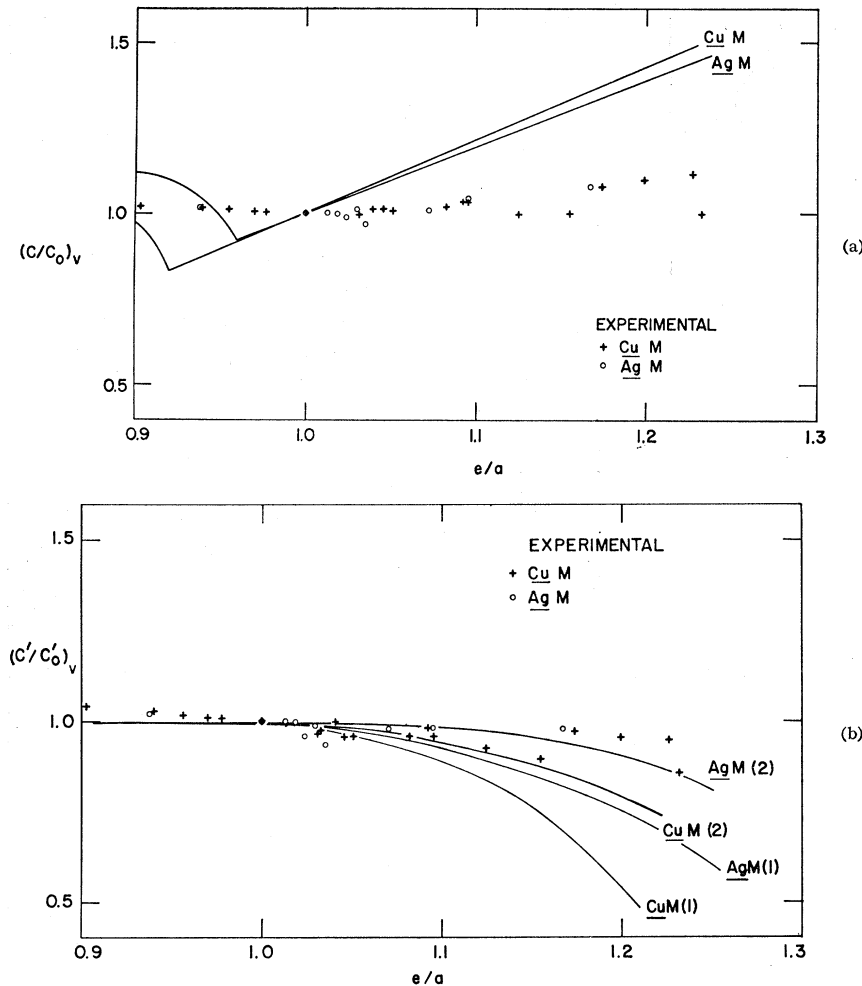


FIG. 6. Reduced elastic shear moduli for α -phase alloys of Cu and of Ag. Curves labeled (1) in Fig. 6(b) are calculated using the mean V_{111} and V_{200} given in Table I, and those labeled (2) use the lower limit for V_{111} and V_{200} to show the sensitivity of C' to the choice of V_{θ} . The experimental points have been scaled to 0°K and corrected to constant volume.

But by this time we have passed the α/β phase boundary for these alloys and the calculation is no longer relevant.

B. Numerical Results for Cu and Ag

Because there do not seem to be any measurements of the shear moduli of gold-based alloys, we confine ourselves now to alloys of Cu and of Ag. In Table II we show how the figures for the repulsive contribution to the shear moduli of the pure metals are obtained by subtracting the theoretical values of the electrostatic plus Fermi terms from the measured values. If the repulsive interaction between a pair of ion cores is assumed to have a Born-Mayer form

$$W_R(r) = A e^{-\alpha(r_0-r)/r_0},$$

where r_0 is the equilibrium nearest-neighbor distance, then we find from Eq. (10) that

$$\text{for copper } A = 0.096 \text{ eV/(ion pair)}, \quad \alpha = 13.68;$$

$$\text{for silver } A = 0.085 \text{ eV/(ion pair)}, \quad \alpha = 14.20.$$

These numbers have no great physical significance, but it is interesting to note that they do fit into the empirical

scheme of A and α values drawn up by Mann and Seeger²⁹ in their survey of a number of methods which have been used to estimate the elastic moduli of copper. We also compare our contributions to C and C' for copper with those of Sinha³⁰ and of Toya,³¹ who screened the bare ion-ion electrostatic interaction with a free-electron gas and so calculated C_{E+F} and C_{E+F}' as a dielectric problem. The entries for C_F and C_F' attributed to these authors in Table II have been found by subtracting Fuchs's value for C_E and C_E' from their total screened-ion contribution and calling the remainder the Fermi term.

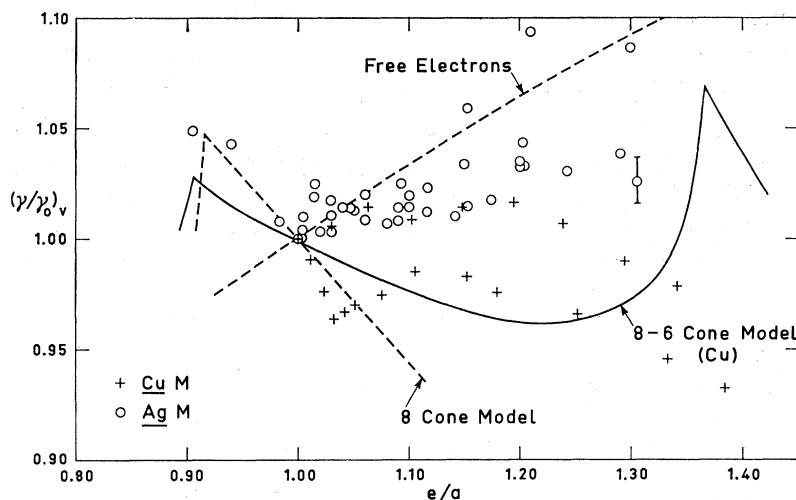
With this choice of C_R and C_R' , all parameters in the calculation are fixed and we can go on to evaluate the shear moduli for x different from one. The results for the Cu and the Ag systems are shown in Fig. 6. We have used C_F and C_F' calculated from our model and have kept C_R and C_R' constant; in the electrostatic terms we

²⁹ E. Mann and A. Seeger, J. Phys. Chem. Solids 12, 314 (1960).

³⁰ S. K. Sinha, Phys. Rev. 143, 422 (1966).

³¹ T. Toya, J. Res. Inst. Catalysis Hokkaido Univ. 9, 178 (1961).

FIG. 7. Relative variation with e/a ratio of the electronic heat capacity for α -phase alloys of Cu and Ag. Experimental points for copper-based alloys (see Refs. 4 and 5) and for silver-based alloys (see Refs. 5-7) have been reduced to constant volume for comparison with theoretical curves of the density of states calculated using the 8-6 cone model (full line), Ziman's 8-cone model (Ref. 9; dashed line), and the free-electron model (dashed line). A typical error bar is shown for one of the more concentrated alloys.



have assumed that the valency Z is equal to x . The curves labeled (1) in Fig. 6(b) have been calculated using the mean values of V_{111} and V_{200} given in Table I, whereas those labeled (2) use the minimum values of V_{111} and V_{200} allowed by the uncertainty in the experimental measurements. The large difference is due primarily to the change in V_{200} , and shows the extreme sensitivity of C_F' to this parameter. On the other hand, the curves for C are quite insensitive to any variation in V_{111} or V_{200} .

The experimental points shown in Fig. 6 for Cu-based alloys¹⁰⁻¹³ and Ag-based alloys¹⁴ have been modified in two ways. Firstly, where the measurements were made at room temperature they have been scaled to 0°K values using the measured ratio for the solvent metals.¹⁴ (Since we are using the harmonic approximation to calculate Θ , we should strictly use a linear extrapolation to 0°K of the high-temperature elastic moduli rather

than the measured low-temperature values, i.e., we should consistently ignore the existence of zero-point energy, but we do not do so because it makes little difference to the numbers obtained.) Secondly, all measurements, which are made at constant pressure, have been corrected to constant volume in keeping with the assumptions of the calculation. If x is the electron/atom ratio, we can write

$$\left(\frac{\partial C}{\partial x}\right)_P = \left(\frac{\partial C}{\partial x}\right)_V + \frac{\partial C}{\partial \ln a} \left(\frac{\partial \ln a}{\partial x}\right)_{x=0}$$

Daniels and Smith³² have measured the change in elastic moduli with pressure for Cu and Ag, and the variation of lattice spacing with composition is known for each of the alloys considered here.¹⁶ Both of these variations are linear and we can write for either C or C'

$$\Delta C_V = \Delta C_P - (\partial C / \partial \ln a) \Delta \ln a,$$

where $\Delta C = C_{\text{alloy}} - C_{\text{solvent}}$. The constant volume correction is important and accounts for the greater part of the observed change in the elastic moduli, so that the final plot of points on a reduced scale shows very little variation from unity.

V. ELECTRONIC HEAT CAPACITY

For completeness we include a plot (Fig. 7) of the ratio of the electronic heat capacities of the alloys γT to those of the pure solvents $\gamma_0 T$ as functions of x . The lines show the density of states calculated (for the copper matrix) using the 8-6 cone model and using the 8-cone model,⁹ and also the density of states for a distribution of free electrons. The experimental points⁴⁻⁷ show the specific heat per mole scaled to the constant molar volume of the solvent metal so as to provide a

TABLE II. Contributions to the elastic shear moduli of pure Cu and Ag. The repulsive term is the difference between the measured value and the sum of the electrostatic and Fermi terms. Units are 10^{11} dyn cm^{-2} .

	C			C'		
	Present	Sinha ^a	Toya ^b	Present	Sinha ^a	Toya ^b
Copper						
Experiment ^c	8.14	8.14	8.14	2.60	2.60	2.60
Electrostat.	2.57	2.57 ^e	2.57 ^e	0.29	0.29 ^e	0.29 ^e
Fermi	-4.25	-0.38 ^e	-2.45 ^e	-0.75	0.06 ^e	0.19 ^e
Repulsive	9.82	5.35	8.02	3.06	2.01	2.12
Silver						
Experiment ^d	5.11	1.71
Electrostat.	1.58	0.18
Fermi	-2.32	-0.35
Repulsive	5.85	1.88

^a Reference 30.

^b Reference 31.

^c Reference 13.

^d Reference 14.

^e Both Sinha and Toya calculated C_{E+F} . We have arbitrarily split this into electrostatic and Fermi terms using Fuchs's results for the electrostatic contribution.

³² W. B. Daniels and C. S. Smith, Phys. Rev. **111**, 713 (1958).

meaningful comparison with the theoretical density-of-states curves, i.e.,

$$(\gamma/\gamma_0)_V = \gamma a_0^2 / \gamma_0 a^2 = (N/N_0)_V.$$

Not a great deal can be said about these results. Even disregarding the low values for one series of CuZn alloys,⁵ there is considerable scatter in the experimental points and none of the theoretical curves represents the observed behavior at all well.

VI. DISCUSSION

A glance at Fig. 6 shows that, given the uncertainty in V_{200} , the calculated values of C' are in reasonable accord with the experimental points, but the calculated C does not agree at all with the measurements. A much larger variation of C with x is predicted than is actually observed and this is due to the predominance of the Fermi term. Because of this poor agreement there is no point in trying to estimate changes in the bulk modulus or in trying to compute the Debye temperature. The most disappointing feature of the whole calculation is that much better agreement with experiment can be obtained^{10,12,24} by completely ignoring the electrons and treating the mean valency and the repulsive term as variables to be fitted to experiment. [A similar treatment applied to $(C_{\text{expt}} - C_F)$ and $(C_{\text{expt}}' - C_F')$ in the present case gave unphysical, negative values for Z^2 .] However, we know that the electrons *must* contribute to the shear moduli for metals whose Fermi surfaces are as distorted as those of the noble metals. We must therefore find out where and why the present calculation has so grossly overestimated the effect of the conduction electrons.

The very rapid increase in C_F with x after contact has been made with the zone boundary is due to a decrease in the density of states N . To agree with the experiments C_F must be a decreasing function of x and N an increasing function of x . We are, in fact, faced with the same dilemma which has arisen in calculations of the electronic heat capacity of these alloy systems: The theoretical density of states decreases for $x > 1$, whereas the experimental results indicate that it should increase more or less as it would for free electrons.

The trouble is probably not due simply to the particular two-plane-wave form of wave function which we have used because C_F seems quite insensitive to precise details of the energy band structure once contact is

made with the zone boundary. It may or may not be due in part to neglect of the d electrons which, although they are several eV below the Fermi surface in the pure metals, do lie right in the center of the conduction band. These could shift on alloying, modify the energy surfaces, and so affect the elastic response of the electrons.

The calculation presupposes the existence of a sharp Fermi surface for these alloys. Little is known yet about the energy bands of alloys or even whether a band structure can be meaningfully defined in such disordered systems. The existence of a reciprocal lattice implies that all unit cells in direct space are identical. But we know from recent work on electron screening that the excess charge introduced by alloying is not spread uniformly among the cells, but is concentrated around the charged impurities. Such a lack of uniformity in direct space leads to a blurring of the electron states in reciprocal space, i.e., to an unsharp Fermi surface. We have assumed not only that a band structure and a sharp Fermi surface exist but also that the bands are rigid, i.e., that the band gaps or Fourier coefficients of the effective potential do not change as the composition changes. This is almost certainly a bad assumption, but we have no experimental knowledge of how the gaps might vary with alloying.

Another assumption which may well be incorrect is that the band gaps are unaffected by shear strains. We know from Templeton's measurements²⁰ of the de Haas-van Alphen effect under pressure that the Fermi surfaces of the noble metals are considerably distorted when the lattice constant is changed, which implies a dependence of the band gaps on volume. Almost certainly they are also shear-strain-dependent, but again we have no experimental evidence for this.

We conclude then that the calculation has failed to account for the observed variation of the shear moduli and hence of the Debye temperature of these Cu- and Ag-based alloys, and that this probably due to the use of a rigid-band model. This type of model now appears unable to explain the behavior of either the electronic or the lattice heat capacity of the α -phase alloys of the noble metals.

ACKNOWLEDGMENTS

I wish to thank J. A. Birch for showing me his specific-heat results prior to publication, and Dr. C. S. Smith for a very helpful discussion about the elastic constants.